

SUPPORTING INFORMATION
accompanying

Copper(II) complexes of a polydentate imidazole-based ligand. pH effect on magnetic coupling and catecholase activity

Edgar Mijangos^a, Jan Reedijk^b, Laura Gasque^{a*}

^a Departamento de Química Inorgánica y Nuclear, Facultad de Química, Universidad Nacional Autónoma de México. Ciudad Universitaria, México D.F. 04510, (México).

^b Leiden Institute of Chemistry, Leiden University. P.O. Box 9502, 2300 RA, Leiden (The Netherlands)

Table of Contents

Figure S1. EPR spectra of 1 and 2 .	2
Figure S2. Diffuse reflectance spectra of 1 and 2 .	2
Figure S3. Possible protonation degrees of the ligand H ₆ Valbiim.	3
Figure S4. Species distribution diagram for H ₆ Valbiim.	3
Figure S5. Changes in chemical shifts of H ₆ Valbiim as function of the pH.	4
Figure S6. Initial rates of H ₂ DTBC oxidation in MeOH/H ₂ O and MeCN/H ₂ O.	5
Figure S7. Lineweaver-Burk plots.	6
Figure S8. CV's of dioxygen in MeOH/H ₂ O and MeCN/H ₂ O.	6
Figure S9. IR spectra of 1 and 2 .	7
Figure S10. UV-Vis titration in MeOH.	7

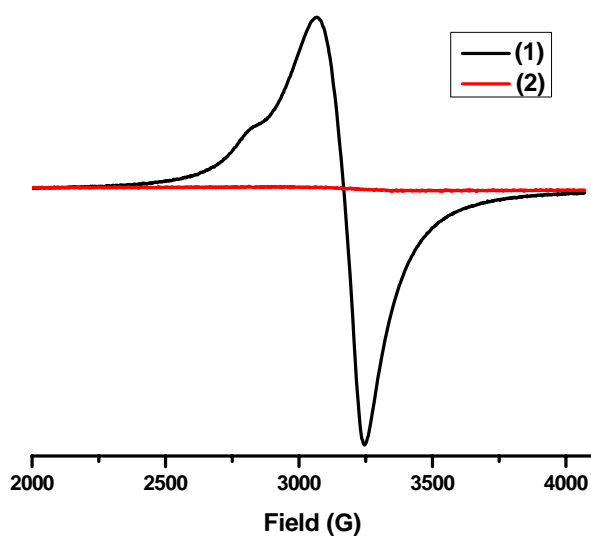


Figure S1. Powder EPR spectra at room temperature of the complexes (Black) **1**, $[\text{Cu}_4(\text{H}_2\text{Valbium})(\text{H}_2\text{O})_{10}](\text{BF}_4)_4 \cdot 6\text{H}_2\text{O}$ and (Red) **2**, $[\text{Cu}_4(\text{Valbium})(\mu\text{-OH})_2(\text{H}_2\text{O})_4] \cdot 5\text{H}_2\text{O}$

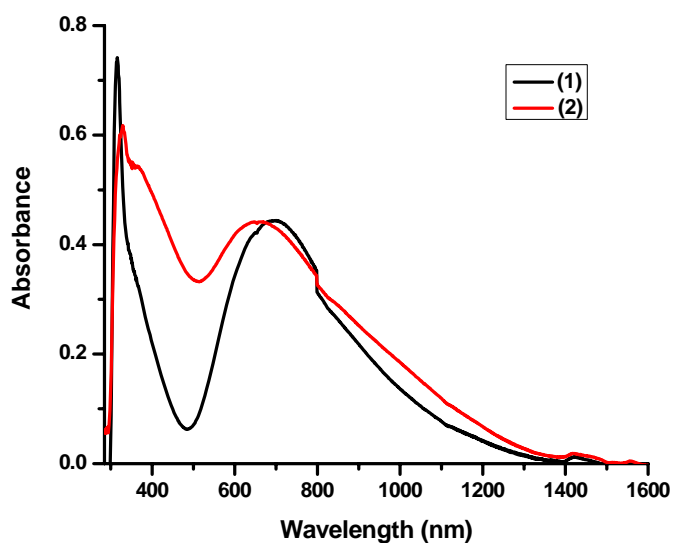


Figure S2. Diffuse reflectance spectra of the complexes (Black) **1**, $[\text{Cu}_4(\text{H}_2\text{Valbium})(\text{H}_2\text{O})_{10}](\text{BF}_4)_4 \cdot 6\text{H}_2\text{O}$ and (Red) **2**, $[\text{Cu}_4(\text{Valbium})(\mu\text{-OH})_2(\text{H}_2\text{O})_4] \cdot 5\text{H}_2\text{O}$. The abnormality near 800 nm is due to change of detector.

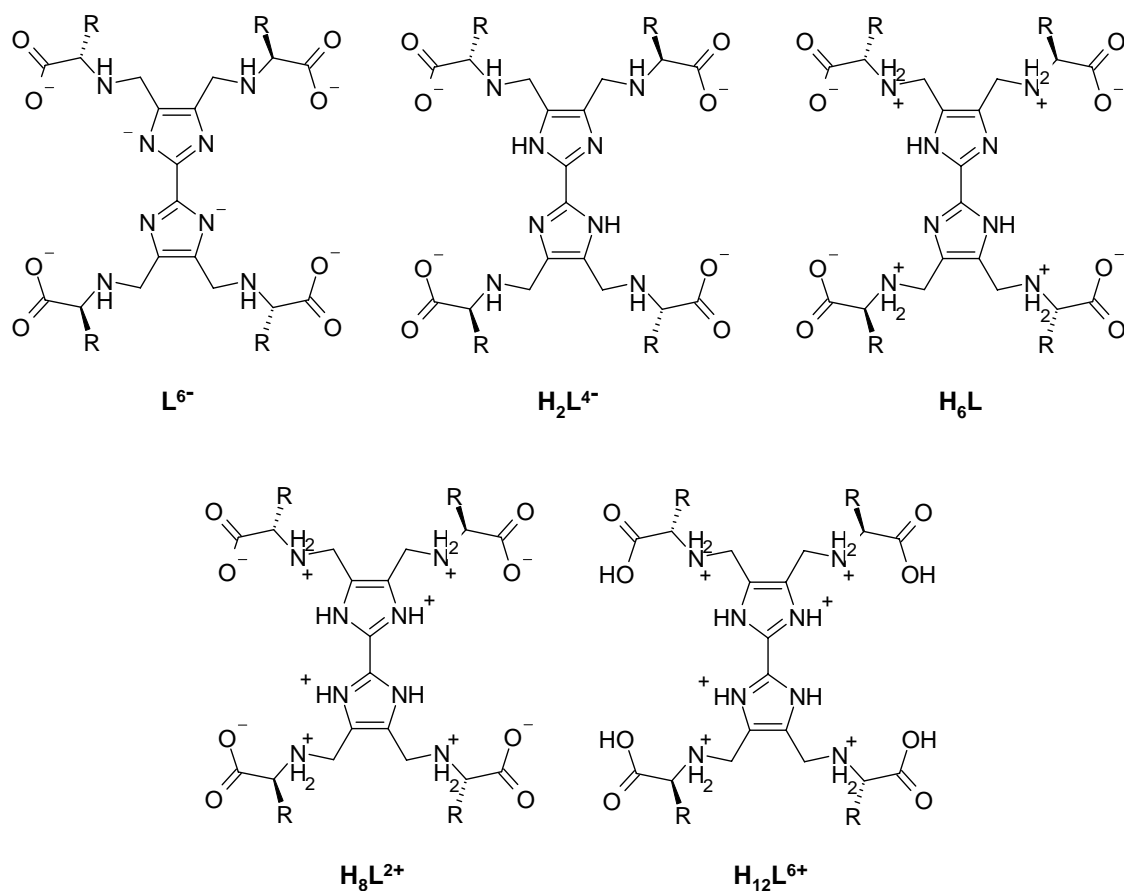


Figure S3. Some of the different possible protonation degrees of the ligand *H₆Valbiim*.

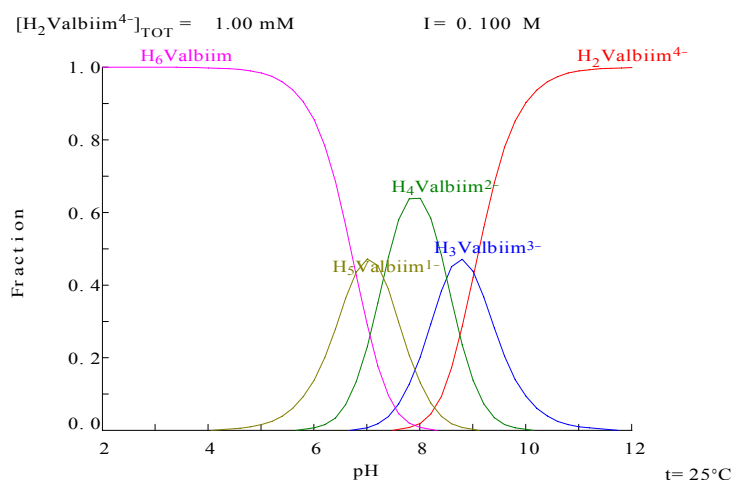


Figure S4. Species distribution diagram as a function of pH for *H₆Valbiim* in aqueous solution.

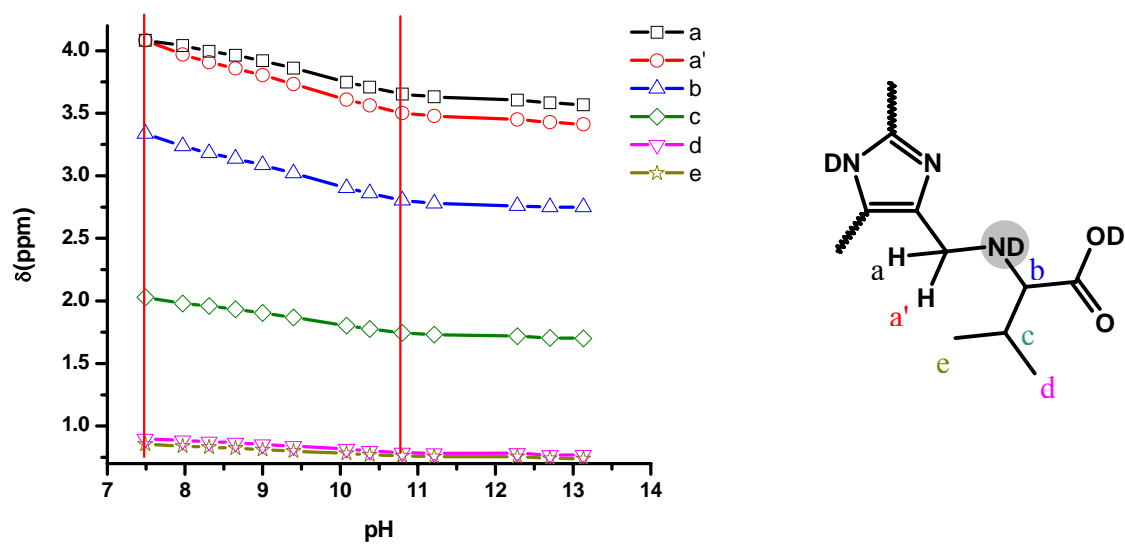


Figure S5. Changes in chemical shifts of selected ^1H NMR signals of H_6Valbim as function of the pH.

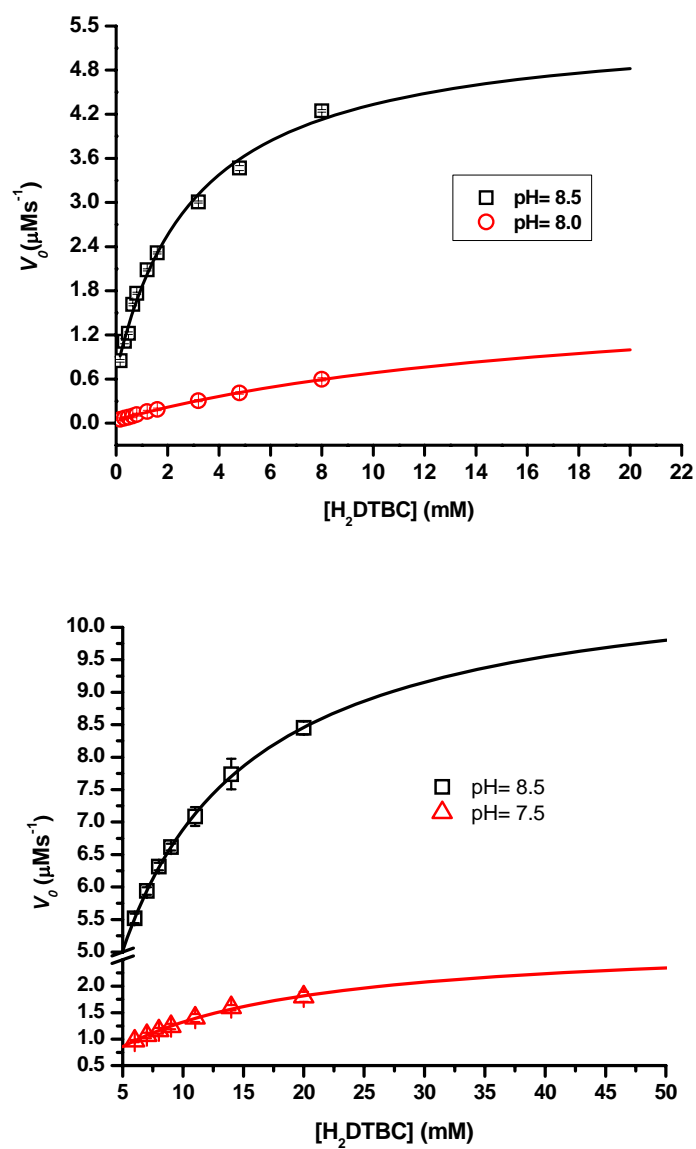


Figure S6. Dependence of the reaction rates on the H_2DTBC concentrations for the oxidation catalyzed by $\text{Cu}_4\text{Valbiim}$ in (up) $\text{MeOH}/\text{H}_2\text{O}$ and (down) $\text{MeCN}/\text{H}_2\text{O}$.

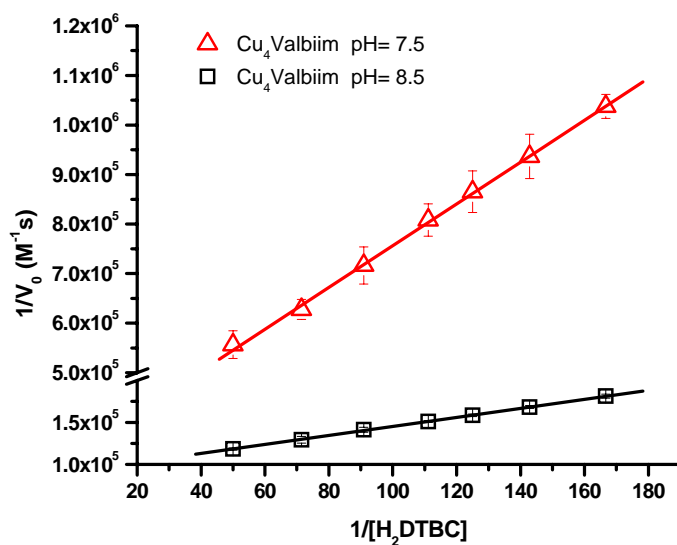


Figure S7. Lineweaver-Burk plot for aerobic oxidation of H_2DTBC by complex $Cu_4Valbiim$ in $MeCN/H_2O$.

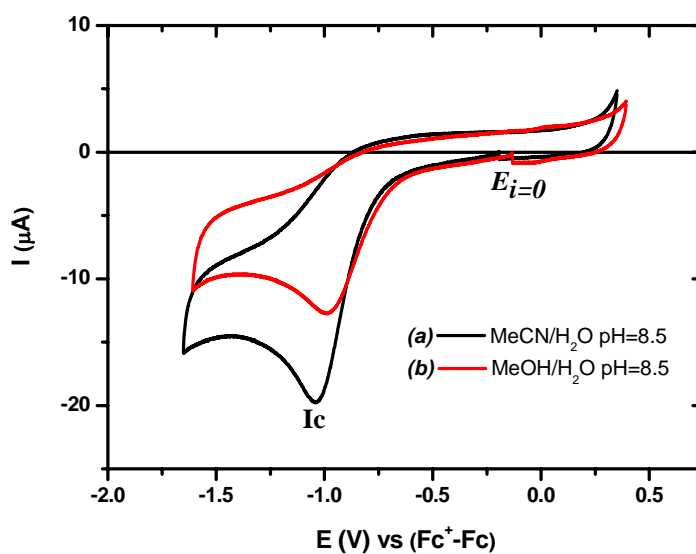


Figure S8. Cyclic voltammograms of atmospheric O_2 saturated solutions of 0.1 M HEPES $pH = 8.5$ in $MeCN/H_2O$; 1:1 (black line) and $MeOH/H_2O$; 1:1 (red line) at 78.1 KPa. Scan rate $0.1 V s^{-1}$. Vitreous carbon disk ($7.1 mm^2$). $Ag/AgBr$, 0.1 M Bu_4NBr reference electrode.

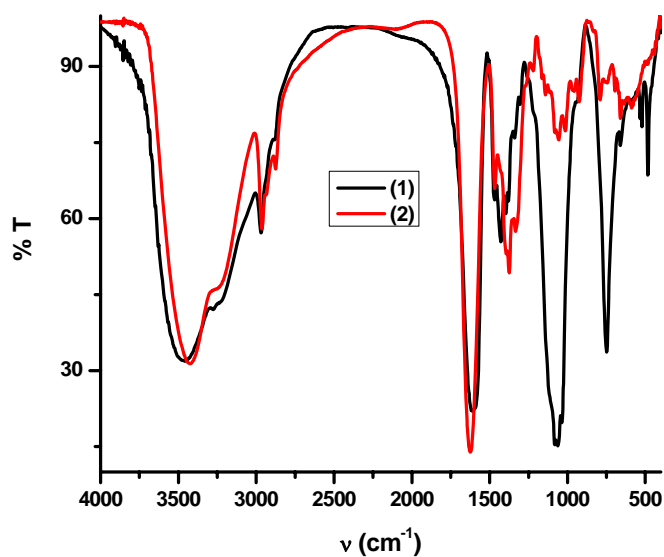


Figure S9. IR spectra of the complexes (Black) **1**, $[\text{Cu}_4(\text{H}_2\text{Valbium})(\text{H}_2\text{O})_{10}](\text{BF}_4)_4 \cdot 6\text{H}_2\text{O}$ and (Red) **2**, $[\text{Cu}_4(\text{Valbium})(\mu\text{-OH})_2(\text{H}_2\text{O})_4] \cdot 5\text{H}_2\text{O}$ in KBr pellet.

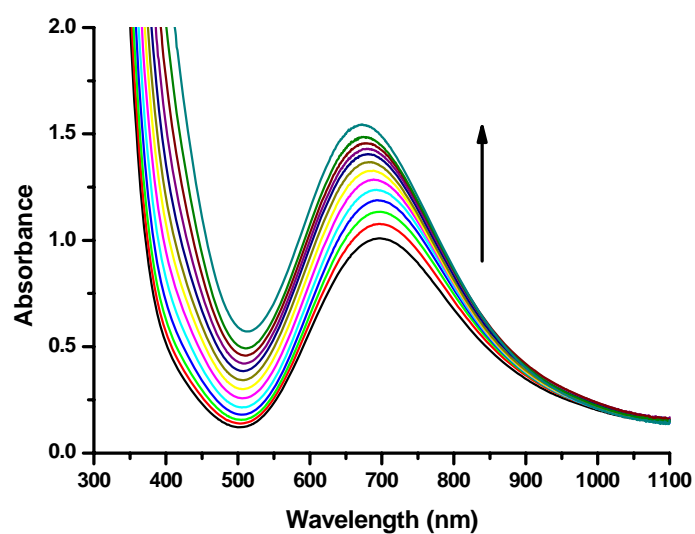


Figure S10. UV-Vis spectra of $[\text{Cu}_4\text{Valbium}]$ (5 mM) in methanol solution at 25 °C as a function of NBu_4OH added. The first line is the spectrum of a solution $4\text{Cu}:\text{H}_6\text{Valbium}$ and the subsequent are the spectra of this solution plus 0.5 to 6 eq.